Inferring demographic and selective histories from population genomic data using a two-step approach in species with coding-sparse genomes: an application to human data

Vivak Soni[1,*] and Jeffrey D. Jensen[1,*]

[1]School of Life Sciences, Center for Evolution & Medicine, Arizona State University, Tempe, AZ, US

[*]Corresponding authors: vsoni11@asu.edu; jeffrey.d.jensen@asu.edu

VS and JDJ conceptualized the project, VS wrote and implemented all code, VS performed the formal analyses with input from JDJ, and VS and JDJ wrote the manuscript. This project was funded by National Institutes of Health grant R35GM139383 to JDJ.

This research was conducted using resources provided by Research Computing at Arizona State University (http://www.researchcomputing.asu.edu) and the Open Science Grid, which is supported by the National Science Foundation and the U.S. Department of Energy's Office of Science.

All authors declare that they have no conflicts of interest.

Code to run simulations and perform analyses is available on GitHub: (https://github.com/vivaksoni/human_demog_DFE/)

Abstract

The demographic history of a population, and the distribution of fitness effects (DFE) of newly arising mutations in functional genomic regions, are fundamental factors dictating both genetic variation and evolutionary trajectories. Although both demographic and DFE inference has been performed extensively in humans, these approaches have generally either been limited to simple demographic models involving a single population, or, where a complex population history has been inferred, without accounting for the potentially confounding effects of selection at linked sites. Taking advantage of the coding-sparse nature of the genome, we propose a 2-step approach in which coalescent simulations are first used to infer a complex multi-population demographic model, utilizing large non-functional regions that are likely free from the effects of background selection. We then use forward-in-time simulations to perform DFE inference in functional regions, conditional on the complex demography inferred and utilizing expected background selection effects in the estimation procedure. Throughout, recombination and mutation rate maps were used to account for the underlying empirical rate heterogeneity across the human genome. Importantly, within this framework it is possible to utilize and fit multiple aspects of the data, and this inference scheme represents a generalized approach for such large-scale inference in species with coding-sparse genomes.

Keywords

demography; distribution of fitness effects; background selection; selective sweeps; genome scans; genetic hitchhiking

Introduction

Genetic variation is a fundamental concern of population genetics. Prior to the advent of next-generation sequencing, the dominant debate within the field was centered on whether levels of genetic variation were expected to be minimal or substantial (known as the *classical/balanced* debate; see Lewontin 1987; Crow 1987). Selection was assumed as the dominant process in both cases, be it purifying selection depressing levels of variation, or balancing selection maintaining polymorphism (Dobzhansky 1955). Despite molecular evidence confirming plentiful levels of genetic variation, Motoo Kimura's Neutral Theory of Molecular Evolution (Kimura 1968, 1983) instead posited that observed variation was largely a consequence of genetic drift; that is, of neutral alleles segregating in the process of drifting towards fixation or loss. This hypothesis – that neutral rather than selective processes can explain the majority of observed variation – has since been largely corroborated (as reviewed in Jensen et al. 2019).

However, quantifying the precise roles of selective and neutral processes in shaping observed levels of variation – and disentangling their individual effects - remains an ongoing challenge due to the similar manners in which multiple evolutionary processes affect patterns of variation. One notable example is the extent to which neutral population growth, background selection (BGS; Charlesworth et al. 1993), and recurrent selective sweeps (Maynard Smith and Haigh 1974) can all skew the site frequency spectrum (SFS, the distribution of allele frequencies) toward rare alleles (Kim 2006; Jensen et al. 2007; Nicolaisen and Desai 2012, 2013; Ewing and Jensen 2016; Johri et al. 2021; Soni et al. 2023; and see review of Charlesworth and Jensen 2021, 2024). The effects of these processes are

72 further modified by genomic heterogeneity in mutation and recombination rates in often
73 complex ways (Soni et al. 2024b). Therefore, if one wishes to quantify the strength and
74 frequency of rare and episodic processes such as positive selection, one must first construct
75 an evolutionarily appropriate baseline model that accounts for the effects of constantly
76 occurring processes including genetic drift as modulated by historical population size
77 changes, as well as the effects of purifying selection and BGS resulting from the removal of
78 deleterious mutations (Bank et al. 2014; Johri et al. 2022a), all whilst accounting for
79 underlying mutation and recombination rate variation. Failure to account for these
80 processes is likely to lead to misinference, particularly in light of the fact that many
81 commonly studied populations and species are thought to have experienced not only
82 population growth, but also recent and severe population bottlenecks [e.g. humans
83 (Gutenkunst et al. 2009; Gravel et al. 2011; Excoffier et al. 2013), non-human primates
84 (Terbot et al. 2024; Soni et al. 2024c) and *Drosophila melanogaster* (Li and Stephan 2006), as
85 well as a variety of human pathogens (Irwin et al. 2016; Sackman et al. 2019; Jensen 2021;
86 Morales-Arce et al. 2021)], a demographic history that is itself often strongly confounded
87 with selective sweeps (Barton 1998; Poh et al. 2014; Matuszewski et al. 2018; Harris and
88 Jensen 2020; Charlesworth and Jensen 2022; Jensen 2023).
89
90 Constructing an evolutionarily appropriate baseline model for a given population will
91 therefore require inferring both a demographic history as well as the distribution of fitness
92 effects (DFE) of new mutations. However, because population history can confound DFE
93 inference, it is necessary to correct for the demographic history of the population in
94 question (Eyre-Walker and Keightley 2007; Boyko et al. 2008). The most commonly used
95 class of approaches are based on a framework in which demographic inference is performed

on putatively neutral sites, before utilizing that demographic history for DFE inference on functional sites (Eyre-Walker and Keightley 2007; Boyko et al. 2008; Galtier 2016; Tataru and Bataillon 2020; and see review of Johri et al. 2022b). Eyre-Walker and Keightley (2007) obtained the first computationally inferred DFE estimates using this approach, and further work incorporated a beneficial class of mutations into the inferred DFE (Boyko et al. 2008; Eyre-Walker and Keightley 2009; Schneider et al. 2011; Galtier 2016).

Notably, this type of 2-step approach is often performed on functional regions under the assumption that all sites are independent and unlinked, and that synonymous sites are selectively neutral. However, these synonymous sites are likely experiencing BGS effects (Charlesworth et al. 1993) due to linkage with directly selected and adjacent non-synonymous sites, resulting in a skew in the SFS and thus mis-inference; in particular, these BGS effects are often misinterpreted as population growth (Ewing and Jensen 2014; Johri et al. 2021; and see review of Johri et al. 2022b). More generally speaking, there is indeed substantial evidence that the effects of selection at linked sites may be widespread across the genomes of many commonly studies species (see reviews of Cutter and Payseur 2013; Charlesworth and Jensen 2021). Although recent work has shown that DFE inference is relatively robust to the biasing effects of selection at linked sites (Kim et al. 2017; Huang et al. 2021), that is not the case for demographic inference (Messer and Petrov 2013; Nicolaisen and Desai 2013; Ewing and Jensen 2016; Schrider et al. 2016; Johri et al. 2021). It is also noteworthy that these 2-step approaches are generally constrained to relatively simple population histories utilizing a two-epoch model (Williamson et al. 2005; Keightley and Eyre-Walker 2007; Kousanthanas and Keightley 2013).

The second class of methods involve using forward-in-time simulations (e.g., in SLiM; Haller and Messer 2023) to jointly and simultaneously infer population history with the DFE in an approximate Bayesian (ABC) framework (see Beaumont et al. 2002), as proposed by Johri et al. (2020). Within this simultaneous inference scheme, it is neither necessary to assume *a priori* the neutrality of synonymous sites, nor is it necessary to assume independence amongst sites; as such, background selection can be directly modelled and incorporated. While 2-step methods commonly infer a continuous distribution for the DFE, this ABC framework infers a number of discrete DFE categories for various ranges of $2N_es$, the population-scaled selection coefficient, where N_e is the effective population size and s is the strength of selection acting on new mutations within the DFE category of interest. The main drawback of such methods is that they are computationally expensive given the large parameter space that must be explored when jointly inferring both demographic and DFE parameters. As such, the inferred demographic models have thus far been limited to single-step size changes in which the ancestral and current population sizes, as well as the timing of size change, are inferred (Johri et al. 2020, 2023). Importantly however, in coding-dense and/or non-recombining species in which sufficiently neutral, unlinked genomic regions may not exist in the genome (thus precluding the needed neutral demographic inference underlying 2-step approaches), this simultaneous inference framework remains the only viable approach (e.g., Howell et al. 2023; Terbot et al. 2023a,b; Soni et al. 2024a).

It thus stands as an outstanding evolutionary inference question of how best to accurately infer a necessarily complex and realistic demographic model, along with a realistic DFE governing functional genomic regions, all whilst accounting for the variety of discussed potential biases. Here we have investigated a modified 2-step approach applied to

144 human populations, in which the population history was inferred using non-functional
145 regions sufficiently distant from functional sites in order to avoid BGS effects, DFE inference
146 was then performed on exonic regions accounting for BGS effects and conditional on the
147 demographic history inferred in Step 1, and mutation and recombination rate maps were
148 utilized to account for the modulating effects of this underlying heterogeneity. By inferring
149 these parameters separately, a more biologically realistic population history was possible
150 accounting for the complexities of population size change, structure, and migration patterns
151 in these studied human populations, while the utilization of these distant non-functional
152 regions allowed for the reduction or elimination of the biasing effects of BGS on
153 demographic inference. Whilst a number of coalescent and diffusion approximation-based
154 approaches would be easily incorporated into our framework (e.g., Gutenkunst et al. 2009;
155 Excoffier et al. 2013; Jouganous et al. 2017; Wang et al. 2020), this approach – like the ABC
156 approach of Johri et al. (2020, 2022a) - has the benefit of utilizing various aspects of
157 population genomic data, including the SFS, associations between variants (linkage
158 disequilibrium, LD), and population differentiation.
159
160 As human populations have naturally been highly studied, with numerous published
161 demographic models, we here provide an optimized and well-fitting 4-population
162 demographic model for the Out-of-Africa (OOA) expansion. Conditional on this model, we
163 additionally optimized a DFE using genic regions, fitting both levels and patterns of
164 polymorphism and divergence, and finding consistency with the recent DFE estimates of
165 Johri et al. (2023). Finally, we have evaluated the degree to which positively selected
166 mutations may be identifiable within the context of this fit model. This work thus provides a

valuable and improved framework for evolutionary inference in coding-sparse genomes, and for the construction of evolutionary baseline models in such species.

Methods and Materials

Data

This study was based on the GRCh37 human reference genome, with SNP data and accessibility masks obtained from 1000 genomes variant call format and bed files, respectively (The 1000 Genomes Project Consortium 2015). The data was split into continental populations, informed by levels of admixture, as determined by The 1000 Genomes Project Consortium (2015). The total number of samples from each of the four considered populations were: African – 99; European – 502; East Asian – 104; South Asian – 489. We obtained recombination and mutation rate maps from Halldorsson et al. (2019) and Francioli et al. (2015), respectively, gene annotations from NCBI (Sayers et al. 2022), ancestral sequences from the six-way EPO alignments available from Ensembl (Flicek et al. 2014; Cunningham et al. 2022), and we identified conserved elements via the 100-way PhastCons score (Siepel et al. 2005; Pollard et al. 2010). See Supplementary Table S1 for links to all downloaded data.

Selecting non-functional regions for demographic inference

For demographic inference we identified non-functional regions of the human genome that were at a distance of at least 10kb from the nearest functional region (as per the NCBI GFF file [Sayers et al. 2022]). We then masked these regions using both strict accessibility masking (The 1000 Genomes Project Consortium 2015) and conserved element

masks (i.e., with a phastCons score > 0 [Siepel et al. 2005; Pollard et al. 2010], in order to remove sites potentially experiencing purifying selection and generating background selection effects (e.g., binding sites (Simkin et al. 2014))). Across each region, we calculated mean recombination and mutation rates, with any regions lacking this information being removed. Finally, we set a minimum length threshold of 15kb to ensure that regions were long enough to reliably calculate summary statistics. Following these steps, we were left with a total of 146 non-functional regions. Finally, we used the B maps of McVicker et al. (2009) to compare the distribution of B values (i.e., the estimated reduction in diversity attributed to BGS by McVicker et al. (2009)) to the distribution of our non-functional regions. For this analysis we lifted over B map coordinates from the hg18 human genome assembly to the GRCh37 assembly using the UCSC liftover tool (Karolchik et al. 2003). Supplementary Figure S1 provides plots of this comparison, as well as the distributions of region lengths, SNPs, and mutation and recombination rates for our set of curated non-functional regions.

Selecting exons for DFE inference

We used the set of exons curated by Johri et al. (2023), although our focus was on the exonic regions only, as opposed to the exons and the neighbouring intergenic regions. Because we used different recombination and mutation rate maps (as described in the data section above), we recalculated mean rates across the 465 exonic regions, removing regions for which we did not have rate information, leaving a total of 397 exonic regions.

Calculating empirical summary statistics

We calculated summary statistics for each population sampled using the python library for libsequence, Pylibseq v0.2.3 (Thornton 2003), except for F_{ST} which was estimated using scikit-allel (Miles et al. 2024). The number of segregating sites and F_{ST} were calculated per site, whilst Tajima's *D* (Tajima 1989) and mean r^2 were calculated over 10kb windows for each non-functional region, and per region for each exon.

Exonic divergence was calculated based on the number of fixed differences between the reference and ancestral sequences, with polymorphic sites masked, relative to total region size.

Calculating summary statistics from simulated data

We calculated summary statistics from simulated data in a manner that replicated the empirical data, using the same software as described above. Thus, sites that had been masked in the empirical data were also masked in the simulated data prior to calculating summary statistics.

Exonic divergence was calculated as the number of fixations post-burn-in from forward-in-time simulations (see the 'Simulating human population history with selection using SLiM' section).

We calculated the mean and standard deviation for each region across its respective 100 replicates. For plotting purposes, we plotted the mean of all regions as the data point, and the mean of the standard deviations across all regions as the confidence intervals.

Simulating human population history using Msprime

Step 1 in our 2-step inference framework was the inference of population history. We simulated human demography using the coalescent simulator Msprime (Baumdicker et al. 2022) for each of our 146 non-functional regions, with region specific mutation and recombination rates. Our demographic model was comprised of 5 populations (four sampled populations: African, European, South Asian and East Asian; as well as the unsampled ancestral Eurasian population) and 25 parameters. Parameter ranges were taken from the human demographic inference literature, with midpoints of all ranges used as the initial starting parameterization. A generation time of 26.9 years was used to appropriately scale simulations (Wang et al. 2023). For details of the demographic model see Figure 1 and Table S2. 100 replicates were simulated for each of the 146 non-functional regions, with a single mutation and recombination rate per region, calculated as the average across the region from the Francioli et al. (2015) mutation rate map and the Halldorsson et al. (2019) recombination rate map (see Supplementary Figure S1 for distributions of region lengths, mutation rates and recombination rates across curated regions). Parameters were optimized to the data using F_{ST}, the number of segregating sites, Tajima's D (Tajima 1989) and mean r^2, across all four populations. Demographic inference plots (e.g., Figure 1) were produced using Demes software (Gower et al. 2022).

Simulating human population history with selection using SLiM

For Step 2, we simulated the inferred population history from Step 1 using the forward-in-time simulator SLiM (v4.0.1 [Haller and Messer 2023]), for our 397 exonic regions, with region specific mutation and recombination rates. We simulated to the

human-chimpanzee split (12mya; Moorjani et al. 2016). Thus, the simulations considered 12 million years (446,100 generations) before starting the 10*N* generation burn-in period. Exonic mutations were drawn from a DFE comprised of 4 fixed classes (following Johri *et al.* 2020), with frequencies denoted by *fi*: f_0 with $0 \leq 2N_{AFRancestral}\, s < 1$ (i.e., effectively neutral mutations), f_1 with $1 \leq 2N_{AFRancestral}\, s < 10$ (i.e., weakly deleterious mutations), f_2 with $10 \leq 2N_{AFRancestral}\, s < 100$ (i.e., moderately deleterious mutations), and f_3 with $100 \leq 2N_{AFRancestral}\, s$ (i.e., strongly deleterious mutations), where $2N_{AFRancestral}$ is the initial African population size and s is the reduction in fitness of the mutant homozygote relative to the wild-type. We initially simulated the DFE from Johri et al. (2023) - comprised of neutral and deleterious mutations - which fit the empirical data well.

Simulating selective sweeps

Recurrent

We simulated recurrent selective sweeps by adding a beneficial DFE category for our 397 exonic regions. We simulated three different beneficial rates (0.1%, 1%, and 10% of new mutations), with the effectively neutral DFE category (f_0) reduced to account for the addition of the beneficial category. Three different beneficial classes were separately simulated: $1 \leq 2N_{AFRancestral}\, s_b < 10$; $10 \leq 2N_{AFRancestral}\, s_b < 100$ and $100 \leq 2N_{AFRancestral}\, s_b < 1{,}000$, where s_b is the increase in mutant homozygote fitness relative to the wild-type.

Individual

To simulate a single hard selective sweep, we ran our inferred demographic model with the inferred DFE, with three different scenarios for introducing a beneficial mutation: model 1) the beneficial mutation was introduced into the African population immediately

after burn-in; model 2) the beneficial mutation was introduced into the ancestral Eurasian population immediately after splitting from the African population; and model 3) the beneficial mutation was introduced into the European population immediately after splitting from the Eurasian population. In model 1, simulations were terminated and restarted if the beneficial mutation did not fix in all 4 sampled populations. In model 2, simulations were terminated and restarted if the hard sweep did not fix in the European, East Asian and South Asian populations. Finally, in model 3 simulations were terminated and restarted if the hard sweep did not fix in the European population. For each scenario, two different strengths of selection were simulated: $2N_e s_b$ = 1,000 and 10,000, where N_e is the ancestral African population size ($N_{AFRancestral}$) and s_b is the beneficial selection coefficient.

For these simulations, we utilized the chromosomal structure of Soni and Jensen (2024), with functional regions comprised of 9 exons (each of size 1,317bp) and 8 introns (each of size 1,520bp), separated by intergenic regions (each of size 4,322bp) [The 1000 Genomes Project Consortium 2015]. The number of exons and introns per functional region were taken from Sakharkar et al. (2004). The chromosomal region contained 7 functional regions in total, resulting in a total simulated region length of 198,345bp.

Variable mutation and recombination rates were drawn from a uniform distribution such that the mean recombination rate across the simulated region for each replicate was equal to the Kong et al. (2010) mean, and the mean mutation rate across the simulated region for each replicate was equal to the Kessler et al. (2020) mean.

311 **Sweep inference with SweepFinder2**

312 We performed selective sweep inference by running SweepFinder2 (DeGiorgio et al.
313 2016) on each simulated replicate of each exonic region from our hard sweep simulations.
314 Allele frequency files were generated for each replicate, following Huber et al.'s (2016)
315 recommendation of including only polymorphic and substitution data. Inference was
316 performed at each SNP via a grid file, following Nielsen et al. (2005). The background SFS
317 was taken from the sweep-free simulations inferred in this study. The following command
318 line was used for inference:
319 SweepFinder2 -lru GridFile FreqFile SpectFile RecFile OutFile
320
321 **Sweep inference with H12**
322 We ran the H12 method of Garud et al. (2015) on each simulated replicate of each
323 exonic region from our hard sweep simulations, using a custom python script. H12 was
324 estimated over 1kb, 2kb, 5kb, 10kb, 20kb, and 40kb windows at each SNP, with the SNP at
325 the center of each window.
326
327 For both SweepFinder2 and H12 inference, we calculated true- and false-positive
328 rates based on the inference values at each site, generating ROC curves from this
329 information.
330
331

Results and Discussion

Our implemented 2-step approach to demographic and DFE inference involves inferring population history using non-functional regions that are at a sufficient distance from functional sites so as to reasonably ensure that they are not experiencing purifying or background selection effects. DFE inference is then performed on exonic regions in Step 2, conditional on the demographic history inferred in Step 1 and incorporating expected background selection effects. We have applied this approach to human population genomic data from the 1000 genomes project (The 1000 Genomes Project Consortium 2015), in order to better characterize the evolutionary parameters governing recent human history.

Step 1: Demographic inference on non-functional regions

In order to avoid the biasing effects of purifying selection and BGS, we performed demographic inference on our curated set of 146 non-functional regions, with mean recombination and mutation rates calculated for each region from the rate maps of Halldorsson et al. (2019) and Francioli et al. (2015), respectively. For details of the data curation steps, please see the Methods section. While one would typically begin with an evaluation of numerous demographic models and topologies in less well-characterized species (see Beaumont et al. 2002; Johri et al. 2020), given the considerable literature on human demographic history (e.g., Gutenkunst et al. 2009; Gravel et al. 2011; Schiffels and Durbin 2014; Terhorst et al. 2017; Hu et al. 2023), and inferred levels of admixture in The 1000 Genomes dataset (The 1000 Genomes Project Consortium 2015), we began with a model of the Out-Of-Africa (OOA) colonization in which the ancestral Eurasian population splits from the African population, followed by the European, South Asian and East Asian

356 populations dispersing from the ancestral Eurasian population, along with the Bantu
357 expansion in the African population. Thus, our demographic model was comprised of 5
358 populations (African, ancestral Eurasian, European, South Asian and East Asian, of which all
359 but the ancestral Eurasian population were sampled) and 25 parameters that capture
360 population sizes, bottleneck severities, growth rates, timings of each event, and migration
361 rates between populations. Parameter ranges were drawn from the extensive literature on
362 human population history (Mellars 2006; Gutenkunst et al. 2009; Gravel et al. 2011;
363 Tennessen et al. 2012; Terhorst et al. 2017). Figure 1a provides the parameter ranges for
364 our model, and see Methods section for further details.
365
366 We simulated 100 replicates for each of our 146 non-functional regions using the
367 coalescent simulator MSprime (Baumdicker et al. 2022) with region-specific mutation and
368 recombination rates, initially starting with midpoint values for each of our parameters (see
369 Figure 1a). For each replicate we estimated four summary statistics for each population (or
370 pairs of populations): the number of segregating sites, Tajima's D (Tajima 1989), mean r^2,
371 and F_{ST}, giving us a total of 18 summary statistics. Fitting these four statistics enabled us to
372 account for multiple aspects of the data including levels of diversity, the SFS, LD and
373 population structure. Figure 1a provides the optimized fit of each parameter within the
374 context of previously published parameter ranges, and Figure 1b the total inferred
375 demographic model. As shown in Figure 2, the summary statistics resulting from this
376 demographic model well fit observed empirical data.
377
378 It is notable that the African population in our model is larger than the African
379 populations in the Gutenkunst et al. (2009) and Gravel et al. (2011) best-fitting models.

There are two likely contributing factors. Firstly, these previous studies fit the model to the SFS, whereas we have here fit multiple diverse summaries of the data. Secondly, these previous studies modeled the African population with a fixed size that undergoes a single instantaneous expansion. Here we modelled the recent Bantu expansion, and thus our final African population size was notably larger, though our final African population size of 87,594 falls within the range of previous estimates (Schiffels and Durbin 2014; Terhorst et al. 2017; Johri et al. 2023). Finally, it is worth noting that numerous other coalescent and diffusion approximation-based approaches have been used to infer the OOA model of human population history (Gutenkunst et al. 2009; Gravel et al. 2011; Excoffier et al. 2013; Jouganous et al. 2017; Wang et al. 2020). These studies have masked genic regions to avoid the biasing effects of selection. However, BGS can still affect demographic inference if not accounted for; nonetheless, our parameter estimates fall within previously inferred ranges, confirming the modest nature of BGS effects in humans (Johri et al. 2021; Buffalo and Kern 2024).

In summary, by optimizing within previously published parameter ranges, we have identified a neutral demographic model that well explains multiple facets of the genomic data in distant non-coding regions.

Step 2: DFE inference on functional regions

Given the strong fit of the neutral demographic model to the intergenic data, we next moved to Step 2: inference of the DFE using functional regions. We utilized the curated set of functional regions from Johri et al. (2023). After obtaining region-specific mutation and recombination rates we were left with a total of 397 functional regions. Unlike Johri et

al. (2023) who simulated exons and their neighboring regions, we focused on the exons only (given that the model fit was consistent across both exons and adjacent regions in their study). First, we simulated our 397 functional regions under the demographic model inferred in Step 1, using the forward-in-time simulator SLiM (v4.0.1 [Haller and Messer 2023]). For the purpose of DFE inference, we simulated to the human-chimpanzee split time (12mya [Moorjani et al. 2016]) to allow us to compare empirical and simulated divergence, which is expected to be shaped by selection at functional sites. When simulating these functional regions under selective neutrality, we found that the fit to the empirical data was poorer than for the non-functional regions (Supplementary Figure S2); an expected result given the action of selection in these exonic regions. Next, we simulated under the Johri et al. (2023) DFE using our fit demographic model, and found a good fit of the simulated summary statistics to the empirical data (Figure 3). These results are encouraging given the differing approaches taken between the two studies: we here took the 2-step approach as described, whilst Johri et al. utilized a simultaneous inference scheme. Importantly however, both studies accounted for expected BGS effects, a relative rarity in DFE inference.

Though the inclusion of population history, purifying and background selection effects, and mutation and recombination rate heterogeneity were alone sufficient to explain empirically observed data patterns, that does not necessarily imply the absence of beneficial mutations; rather, it suggests that this additional parameter is not needed in order to fit observed patterns of variation. While this observation is itself meaningful, it indeed raises the question of what rate of beneficial mutation may be consistent with the data but simply unidentifiable. In order to investigate this question, we added a beneficial DFE category to the Johri et al. (2023) DFE, in an attempt to understand what rate of input of beneficial

mutations may be compatible with the observed levels of variation, the SFS, LD, divergence and F_{ST}. Initially, we considered three beneficial DFE proportions, f_{bo} = [0.1%, 1%, or 10% of newly arising mutations], with $1 \leq 2N_{AFRancestral}\, s_b < 10$ (i.e., weakly beneficial mutations). Under this model, we correspondingly reduced f_0 - the proportion of effectively neutral mutations – in order to account for the addition of this beneficial DFE class. Supplementary Figures S3-S5 provide the fit of the summary statistics from these simulations to the observed data. At f_{b0} = 0.1% or 1%, all summary statistics remain reasonably well fit - in other words, they are not significantly modified from the expectations in the absence of positive selection. However, divergence was notably increased relative to that observed at f_{b0} = 10%, due to the greater rate of beneficial fixation.

Given that this beneficial mutation rate of 10% appears inconsistent with empirical divergence, we next examined f_{b0} = 0.1% and 1% only, whilst increasing the population-scaled strength of selection to $10 \leq 2N_{AFRancestral}\, s_b < 100$ (i.e., moderately beneficial mutations). Supplementary Figures S6 and S7 provide the fit of summary statistics from these simulations to the observed data. With this increased strength of selection, the modelled divergence only fit the empirical data at the lowest beneficial frequency, f_{B0} = 0.1%. Finally, we increased the population-scaled strength of selection further to $100 \leq 2N_{AFRancestral}\, s_b < 1000$ (i.e., strongly beneficial mutations), at f_{B0} = 0.1%. Even at this low frequency, the resulting divergence was too high relative to the empirical data (see Supplementary Figure S8 for all summary statistics). It is notable that regardless of beneficial mutation frequency or strength of selection, the other summary statistics fit the data well - this owes to the relative waiting time between selective sweeps under these models; that is, selective sweeps are too old on average to strongly impact patterns of polymorphism

(Jensen 2009), while being frequent enough to modify divergence over the 12mya time-scale.

Taken together, these results suggest that whilst the addition of a beneficial DFE class is not necessary to explain the patterns observed in the human population genomic data here considered, a modest input of weakly beneficial mutations and/or a low input of moderately beneficial mutations would remain consistent with the observed data.

Evaluating power to detect selective sweeps within this human baseline model

Recurrent sweep models, such as the one studied above, involve a scenario in which beneficial mutations occur randomly across a chromosome according to a time-homogenous Poisson process at a per-generation rate (Kaplan et al. 1989; Wiehe and Stephan 1993; Stephan 1995; Pavlidis et al. 2010; Soni et al. 2023). Although this is a more realistic model of positive selection, in that the beneficial mutations underlying selective sweeps naturally occur at a per-generation rate - meaning that they are naturally associated with an average time since fixation - the more commonly studied model involves a single selective sweep in which fixation occurred immediately prior to sampling. As such, these models consider a best-case scenario for sweep detection, both in that sweeps are as recent as possible thus maximizing detectable polymorphism-based patterns (see review of Nielsen 2005), but also because it avoids the possibility of interference between positively selected mutations (i.e., Hill and Robertson 1966).

Furthermore, these models are often simulated on otherwise neutral backgrounds, which is additionally unrealistic in the sense that beneficial mutations occur in functional regions, which will be dominated by newly arising deleterious mutations. Thus, as a step

476 towards biological reality, we here have modelled single selective sweeps within the context
477 of our evolutionary baseline model, using our inferred demographic history, DFE, as well as
478 mutation and recombination rate maps, thereby accounting for constantly-operating
479 evolutionary processes in order to characterize the power to identify an episodic selective
480 sweep (as described by Johri et al. 2022a).
481
482 Under this model, we simulated a large genomic region comprised of functional and
483 non-functional regions in which a single hard selective sweep occurred in a functional
484 element (see Methods section for more details about simulated chromosomal structure, as
485 well as parameterizations). Sweep inference was conducted using two methods: the
486 composite-likelihood ratio (CLR) SFS-based method, SweepFinder2 (DeGiorgio et al. 2016),
487 and a haplotype-based approach, H12. Three different sweep models were simulated: 1) a
488 beneficial mutation introduced into the ancestral African population immediately after
489 simulation burn-in, with the fixed beneficial present in the sampled African, European, East
490 Asian and South Asian populations; 2) a beneficial mutation introduced into the ancestral
491 Eurasian population immediately after splitting from the ancestral African population, with
492 the fixed beneficial present in the sampled European, East Asian and South Asian
493 populations; and 3) a beneficial mutation introduced into the European population
494 immediately after splitting from the Eurasian population, with the fixed beneficial present in
495 the sampled European population. Figure 4 presents ROC plots, plotting the false positive
496 rate (FPR) against the true positive rate (TPR) for inference on each model across 100
497 replicates with SweepFinder2 (with inference performed at each SNP) and H12 (with
498 inference performed across 1kb windows, centered on each SNP; see Supplementary
499 Figures S9-13 for additional window sizes).

At the lowest strength of selection ($2N_e s_b = 100$), no beneficial mutations reached fixation by the sampling time (i.e., the present day) across the replicates. As such, Figure 4 presents ROC plots for $2N_e s_b$ values of 1,000 and 10,000 only. Although SweepFinder2 showed greater inference power than H12, there was limited power to detect selective sweeps for both approaches. While potentially appearing counter-intuitive, in some circumstances $2N_e s_b$ = 1,000 had greater power than $2N_e s_b$ = 10,000, as the fixations of the former were more recent given the longer sojourn time, and thus experienced less post-fixation decay in patterns of polymorphism (Kim and Stephan 2000; Soni et al. 2023). These results thus suggest that detectable selective sweeps would necessarily be the result of positive selection that was strong and recent enough to leave a detectable signature, consistent with previous work (Przeworski 2002; Kim and Stephan 2002; Jensen et al. 2007; Crisci et al. 2013). Moreover, the modest power under our baseline model is likely explained by the severe bottlenecks and expansions characterizing these populations, as the fundamental difficulty in distinguishing between population bottlenecks and selective sweeps has been previously demonstrated (Barton 1998; Jensen et al. 2005). These results suggest that caution is needed when performing genomic scans for selection in humans due to their complex recent demographic history, and likely supports previous assertions that strong selective sweeps have been rare in recent human history (Hernandez et al. 2011).

Conclusions

In this study we have demonstrated the viability of a 2-step approach for inferring population history along with the DFE in coding-sparse genomes, such as that characterizing humans. This condition, together with being a recombining genome, is important for the

existence and availability of non-functional regions sufficiently distant from functional sites so as to be free from the effects of purifying and background selection, as such regions are necessary for the accurate inference of population history. By contrast, organisms with genomes that are either coding dense or experience limited recombination may not have such regions in sufficient number, in which case demographic inference must be performed within the context of background selection effects. As these background selection effects will be dictated partially by the DFE in functional regions, this genomic architecture requires the joint and simultaneous inference of demographic and selective parameters - a situation that spans organisms ranging from *Drosophila* to many viruses (see review of Johri et al. 2022b). However, given the multiple jointly inferred parameters, the demographic histories under these joint inference schemes have been highly simplified in current implementations. Thus, this 2-step approach has a distinct advantage for coding-sparse genomes, in that previously developed and sophisticated neutral demographic inference approaches may be leveraged in Step 1 - such as that employed here estimating a 25-parameter human demographic model consisting of multiple population size changes, split times, and migration rates - allowing DFE inference to be focused upon in Step 2 conditional on that inferred history.

It is additionally important to consider the extent to which a consideration of these BGS effects matters for human demographic inference. Indeed, given the coding-sparseness of the genome, these effects are expected *a priori* to be limited, and that is fully consistent with the observation that our optimized demographic parameter values fall within previously published parameter ranges. However, apart from accounting for the effects of selection at linked sites, this approach also utilizes patterns of variation in addition to the site frequency spectrum (e.g., linkage disequilibrium and population-differentiation), which

provide a further valuable 'sanity check' on estimated models. This combination of factors has resulted in incrementally improved - but indeed improved - parameter estimates for the populations studied, as assessed by the fit between the estimated model and the empirical data. Thus, this proof-of-principle approach applied here to publicly-available human data will likely provide a highly relevant and informative inference framework for the analysis of future genomic resources in comparatively poorly-studied species with a similar genomic architecture (e.g., non-human primates).

References

Bank, C., Ewing, G. B., Ferrer-Admettla, A., Foll, M., & Jensen, J. D. (2014). Thinking too positive? Revisiting current methods of population genetic selection inference. *Trends in Genetics*, *30*(12), 540–546. https://doi.org/10.1016/j.tig.2014.09.010

Barton, N. H. (1998). The effect of hitch-hiking on neutral genealogies. *Genetical Research*, *72*(2), 123–133. https://doi.org/10.1017/S0016672398003462

Baumdicker, F., Bisschop, G., Goldstein, D., Gower, G., Ragsdale, A. P., Tsambos, G., Zhu, S., Eldon, B., Ellerman, E. C., Galloway, J. G., Gladstein, A. L., Gorjanc, G., Guo, B., Jeffery, B., Kretzschumar, W. W., Lohse, K., Matschiner, M., Nelson, D., Pope, N. S., … Kelleher, J. (2022). Efficient ancestry and mutation simulation with msprime 1.0. *Genetics*, *220*(3), iyab229. https://doi.org/10.1093/genetics/iyab229

Beaumont, M. A., Zhang, W., & Balding, D. J. (2002). Approximate Bayesian Computation in population genetics. *Genetics*, *162*(4), 2025–2035. https://doi.org/10.1093/genetics/162.4.2025

Boyko, A. R., Williamson, S. H., Indap, A. R., Degenhardt, J. D., Hernandez, R. D., Lohmueller, K. E., Adams, M. D., Schmidt, S., Sninsky, J. J., Sunyaev, S. R., White, T. J., Nielsen, R., Clark, A. G., & Bustamante, C. D. (2008). Assessing the evolutionary impact of amino acid mutations in the human genome. *PLoS Genetics*, *4*(5), e1000083. https://doi.org/10.1371/journal.pgen.1000083

Buffalo, V., & Kern, A. D. (2024). A quantitative genetic model of background selection in humans. *PLOS Genetics*, *20*(3), e1011144. https://doi.org/10.1371/journal.pgen.1011144

Charlesworth, B., & Jensen, J. D. (2021). Effects of selection at linked Sites on patterns of genetic variability. *Annual Review of Ecology, Evolution, and Systematics*, *52*(1), 177–197. https://doi.org/10.1146/annurev-ecolsys-010621-044528

Charlesworth, B., & Jensen, J.D. (2022). Some complexities in interpreting apparent effects of hitchhiking: a commentary on Gompert *et al.* 2022. *Molecular Ecology,* 31, 4440-4443. https://doi.org/10.1111/mec.16573

Charlesworth, B., & Jensen, J.D. (2024). Population genetics. *Encyclopedia of Biodiversity, 3rd ed.* Elsevier Ltd. Vol. 7: 467-483.

Charlesworth, B., Morgan, M. T., & Charlesworth, D. (1993). The effect of deleterious mutations on neutral molecular variation. *Genetics*, *134*(4), 1289–1303.

Crisci, J. L., Poh, Y.-P., Mahajan, S., & Jensen, J. D. (2013). The impact of equilibrium assumptions on tests of selection. *Frontiers in Genetics*, *4*. https://doi.org/10.3389/fgene.2013.00235

Crow, J. F. (1987). Muller, Dobzhansky, and overdominance. *Journal of the History of Biology*, *20*(3), 351–380. https://doi.org/10.1007/BF00139460

Cunningham, F., Allen, J. E., Allen, J., Alvarez-Jarreta, J., Amode, M. R., Armean, I. M., Austine-Orimoloye, O., Azov, A. G., Barnes, I., Bennett, R., Berry, A., Bhai, J., Bignell, A., Billis, K., Boddu, S., Brooks, L., Charkhchi, M., Cummins, C., Da Rin Fioretto, L., … Flicek, P. (2022). Ensembl 2022. *Nucleic Acids Research*, *50*(D1), D988–D995. https://doi.org/10.1093/nar/gkab1049

Cutter, A. D., & Payseur, B. A. (2013). Genomic signatures of selection at linked sites: Unifying the disparity among species. *Nature Reviews. Genetics*, *14*(4), 262–274. https://doi.org/10.1038/nrg3425

619 Dobzhansky T. 1955. A review of some fundamental concepts and problems of population
620 genetics. Cold Spring Harb Symp Quant Biol. 20:1–15.
621 doi:10.1101/SQB.1955.020.01.003.
622 DeGiorgio, M., Huber, C. D., Hubisz, M. J., Hellmann, I., & Nielsen, R. (2016). SweepFinder2:
623 Increased sensitivity, robustness and flexibility. *Bioinformatics*, *32*(12), 1895–1897.
624 https://doi.org/10.1093/bioinformatics/btw051
625 Ewing, G. B., & Jensen, J. D. (2014). Distinguishing neutral from deleterious mutations in
626 growing populations. *Frontiers in Genetics*, *5*.
627 https://doi.org/10.3389/fgene.2014.00007
628 Ewing, G. B., & Jensen, J. D. (2016). The consequences of not accounting for background
629 selection in demographic inference. *Molecular Ecology*, *25*(1), 135–141.
630 https://doi.org/10.1111/mec.13390
631 Excoffier, L., Dupanloup, I., Huerta-Sánchez, E., Sousa, V. C., & Foll, M. (2013). Robust
632 demographic inference from genomic and SNP data. *PLoS Genetics*, *9*(10), e1003905.
633 https://doi.org/10.1371/journal.pgen.1003905
634 Eyre-Walker, A., & Keightley, P. D. (2009). Estimating the Rate of Adaptive Molecular
635 Evolution in the Presence of Slightly Deleterious Mutations and Population Size
636 Change. *Molecular Biology and Evolution*, *26*(9), 2097–2108.
637 https://doi.org/10.1093/molbev/msp119
638 Eyre-Walker, A., & Keightley, P. D. (2007). The distribution of fitness effects of new
639 mutations. *Nature Reviews Genetics*, *8*(8), 610–618. https://doi.org/10.1038/nrg2146
640 Flicek, P., Amode, M. R., Barrell, D., Beal, K., Billis, K., Brent, S., Carvalho-Silva, D., Clapham,
641 P., Coates, G., Fitzgerald, S., Gil, L., Girón, C. G., Gordon, L., Hourlier, T., Hunt, S.,
642 Johnson, N., Juettemann, T., Kähäri, A. K., Keenan, S., … Searle, S. M. J. (2014). Ensembl
643 2014. *Nucleic Acids Research*, *42*(D1), D749–D755.
644 https://doi.org/10.1093/nar/gkt1196
645 Francioli, L. C., Polak, P. P., Koren, A., Menelaou, A., Chun, S., Renkens, I., Genome of the
646 Netherlands Consortium, van Duijn, C. M., Swertz, M., Wijmenga, C., van Ommen, G.,
647 Slagboom, P. E., Boomsma, D. I., Ye, K., Guryev, V., Arndt, P. F., Kloosterman, W. P., de
648 Bakker, P. I. W., & Sunyaev, S. R. (2015). Genome-wide patterns and properties of de
649 novo mutations in humans. *Nature Genetics*, *47*(7), 822–826.
650 https://doi.org/10.1038/ng.3292
651 Galtier, N. (2016). Adaptive protein evolution in animals and the effective population size
652 Hypothesis. *PLOS Genetics*, *12*(1), e1005774.
653 https://doi.org/10.1371/journal.pgen.1005774
654 Garud, N. R., Messer, P. W., Buzbas, E. O., & Petrov, D. A. (2015). Recent selective sweeps in
655 North American *Drosophila melanogaster* show signatures of soft sweeps. *PLOS*
656 *Genetics*, *11*(2), e1005004. https://doi.org/10.1371/journal.pgen.1005004
657 Gower, G., Ragsdale, A. P., Bisschop, G., Gutenkunst, R. N., Hartfield, M., Noskova, E.,
658 Schiffels, S., Struck, T. J., Kelleher, J., & Thornton, K. R. (2022). Demes: A standard
659 format for demographic models. *Genetics*, *222*(3), iyac131.
660 https://doi.org/10.1093/genetics/iyac131
661 Gravel, S., Henn, B. M., Gutenkunst, R. N., Indap, A. R., Marth, G. T., Clark, A. G., Yu, F.,
662 Gibbs, R. A., The 1000 Genomes Project, Bustamante, C. D., Altshuler, D. L., Durbin, R.
663 M., Abecasis, G. R., Bentley, D. R., Chakravarti, A., Clark, A. G., Collins, F. S., De La Vega,
664 F. M., Donnelly, P., … McVean, G. A. (2011). Demographic history and rare allele sharing

665 among human populations. *Proceedings of the National Academy of Sciences*, *108*(29),
666 11983–11988. https://doi.org/10.1073/pnas.1019276108
667 Gutenkunst, R. N., Hernandez, R. D., Williamson, S. H., & Bustamante, C. D. (2009). Inferring
668 the Joint demographic history of multiple populations from multidimensional SNP
669 frequency data. *PLoS Genetics*, *5*(10), e1000695.
670 https://doi.org/10.1371/journal.pgen.1000695
671 Halldorsson, B. V., Palsson, G., Stefansson, O. A., Jonsson, H., Hardarson, M. T., Eggertsson,
672 H. P., Gunnarsson, B., Oddsson, A., Halldorsson, G. H., Zink, F., Gudjonsson, S. A.,
673 Frigge, M. L., Thorleifsson, G., Sigurdsson, A., Stacey, S. N., Sulem, P., Masson, G.,
674 Helgason, A., Gudbjartsson, D. F., … Stefansson, K. (2019). Characterizing mutagenic
675 effects of recombination through a sequence-level genetic map. *Science*, *363*(6425),
676 eaau1043. https://doi.org/10.1126/science.aau1043
677 Haller, B. C., & Messer, P. W. (2023). SLiM 4: Multispecies eco-evolutionary modeling. *The*
678 *American Naturalist*, *201*(5), E127–E139. https://doi.org/10.1086/723601
679 Harris, R. B., & Jensen, J. D. (2020). Considering genomic scans for selection as coalescent
680 model choice. *Genome Biology and Evolution*, *12*(6), 871–877.
681 https://doi.org/10.1093/gbe/evaa093
682 Henn, B. M., Botigué, L. R., Peischl, S., Dupanloup, I., Lipatov, M., Maples, B. K., Martin, A. R.,
683 Musharoff, S., Cann, H., Snyder, M. P., Excoffier, L., Kidd, J. M., & Bustamante, C. D.
684 (2016). Distance from sub-Saharan Africa predicts mutational load in diverse human
685 genomes. *Proceedings of the National Academy of Sciences*, *113*(4), E440–E449.
686 https://doi.org/10.1073/pnas.1510805112
687 Hernandez, R.D., Kelley, J.L., Elyashiv, E., Melton, S.C., Auton, A., McVean, G., 1000 Genomes
688 Project, Sella, G., & Przeworski, M. (2011). Classic selective sweeps were rare in recent
689 human evolution. *Science*, 331(6019), 920-924.
690 https://doi.org/10.1126/science.1198878
691 Hill, W. G., & Robertson, A. (1966). The effect of linkage on limits to artificial selection.
692 *Genetical Research*, *8*(3), 269–294.
693 Howell, A.A., Terbot, J., Soni, V., Johri, P., Jensen, J.D., & Pfeifer, S.P. (2023). Developing an
694 appropriate evolutionary baseline model for the study of human cytomegalovirus.
695 *Genome Biology and Evolution,* 15, evad059.
696 https://doi.org/10.1093/gbe/evad059
697 Hu, W., Hao, Z., Du, P., Di Vincenzo, F., Manzi, G., Cui, J., Fu, Y.-X., Pan, Y.-H., & Li, H. (2023).
698 Genomic inference of a severe human bottleneck during the Early to Middle
699 Pleistocene transition. *Science*, *381*(6661), 979–984.
700 https://doi.org/10.1126/science.abq7487
701 Huang, X., Fortier, A. L., Coffman, A. J., Struck, T. J., Irby, M. N., James, J. E., León-Burguete,
702 J. E., Ragsdale, A. P., & Gutenkunst, R. N. (2021). Inferring genome-wide correlations of
703 mutation fitness effects between populations. *Molecular Biology and Evolution*, *38*(10),
704 4588–4602. https://doi.org/10.1093/molbev/msab162
705 Huber, C. D., DeGiorgio, M., Hellmann, I., & Nielsen, R. (2016). Detecting recent selective
706 sweeps while controlling for mutation rate and background selection. *Molecular*
707 *Ecology*, *25*(1), 142–156. https://doi.org/10.1111/mec.13351
708 Irwin, K. K., Laurent, S., Matuszewski, S., Vuilleumier, S., Ormond, L., Shim, H., Bank, C., &
709 Jensen, J. D. (2016). On the importance of skewed offspring distributions and
710 background selection in virus population genetics. *Heredity*, *117*(6), 393–399.
711 https://doi.org/10.1038/hdy.2016.58

712 Jensen, J.D. (2009). On reconciling single and recurrent hitchhiking models. *Genome Biology*
713 *and Evolution,* 1, 320-324.
714 https://doi.org/10.1093/gbe/evp031
715 Jensen, J. D. (2021). Studying population genetic processes in viruses: From drug-resistance
716 evolution to patient infection dynamics. *Encyclopedia of Virology* (pp. 227–232).
717 Elsevier. https://doi.org/10.1016/B978-0-12-814515-9.00113-2
718 Jensen, J.D. (2023). Population genetic concerns related to the interpretation of empirical
719 outliers and the neglect of common evolutionary processes. *Heredity,* 130, 109-110.
720 https://doi.org/10.1038/s41437-022-00575-5
721 Jensen, J.D., Kim, Y., Bauer DuMont, V., Aquadro, C.F., & Bustamante, C.D. (2005).
722 Distinguishing between selective sweeps and demography using DNA polymorphism
723 data. *Genetics*, 170, 1401-1410.
724 https://doi.org/10.1534/genetics.104.038224
725 Jensen, J. D., Payseur, B. A., Stephan, W., Aquadro, C. F., Lynch, M., Charlesworth, D., &
726 Charlesworth, B. (2019). The importance of the Neutral Theory in 1968 and 50 years
727 on: A response to Kern and Hahn 2018: COMMENTARY. *Evolution*, *73*(1), 111–114.
728 https://doi.org/10.1111/evo.13650
729 Jensen, J. D., Thornton, K. R., Bustamante, C. D., & Aquadro, C. F. (2007). On the utility of
730 linkage disequilibrium as a statistic for identifying targets of positive selection in
731 nonequilibrium populations. *Genetics*, *176*(4), 2371–2379.
732 https://doi.org/10.1534/genetics.106.069450
733 Johri, P., Aquadro, C. F., Beaumont, M., Charlesworth, B., Excoffier, L., Eyre-Walker, A.,
734 Keightley, P. D., Lynch, M., McVean, G., Payseur, B. A., Pfeifer, S. P., Stephan, W., &
735 Jensen, J. D. (2022a). Recommendations for improving statistical inference in
736 population genomics. *PLOS Biology*, *20*(5), e3001669.
737 https://doi.org/10.1371/journal.pbio.3001669
738 Johri, P., Charlesworth, B., & Jensen, J. D. (2020). Toward an evolutionarily appropriate null
739 model: Jointly inferring demography and purifying selection. *Genetics*, *215*(1), 173–192.
740 https://doi.org/10.1534/genetics.119.303002
741 Johri, P., Eyre-Walker, A., Gutenkunst, R. N., Lohmueller, K. E., & Jensen, J. D. (2022b). On
742 the prospect of achieving accurate joint estimation of selection with population history.
743 *Genome Biology and Evolution*, *14*(7), evac088. https://doi.org/10.1093/gbe/evac088
744 Johri, P., Pfeifer, S. P., & Jensen, J. D. (2023). Developing an evolutionary baseline model for
745 humans: Jointly inferring purifying selection with population history. *Molecular Biology*
746 *and Evolution*, *40*(5), msad100. https://doi.org/10.1093/molbev/msad100
747 Johri, P., Riall, K., Becher, H., Excoffier, L., Charlesworth, B., & Jensen, J. D. (2021). The
748 impact of purifying and background selection on the inference of population history:
749 Problems and prospects. *Molecular Biology and Evolution*, *38*(7), 2986–3003.
750 https://doi.org/10.1093/molbev/msab050
751 Jouganous, J., Long, W., Ragsdale, A. P., & Gravel, S. (2017). Inferring the Joint Demographic
752 History of Multiple Populations: Beyond the Diffusion Approximation. *Genetics*, *206*(3),
753 1549–1567. https://doi.org/10.1534/genetics.117.200493
754 Kaplan, N. L., Hudson, R. R., & Langley, C. H. (1989). The 'hitchhiking effect' revisited.
755 *Genetics*, *123*(4), 887–899. https://doi.org/10.1093/genetics/123.4.887
756 Karolchik, D., Baertsch, R., Diekhans, M., Furey, T.S., Hinrichs, A., Lu, Y.T., Roskin, K.M.,
757 Schwartz, M., Sugnet, C.W., Thomas, D.J., et al. (2003). The UCSC Genome Browser
758 Database. Nucleic Acids Res. 31: 51–54.

759 Keightley, P. D., & Eyre-Walker, A. (2007). Joint inference of the distribution of fitness
760 effects of deleterious mutations and population demography based on nucleotide
761 polymorphism Frequencies. *Genetics*, *177*(4), 2251–2261.
762 https://doi.org/10.1534/genetics.107.080663
763 Kessler, M. D., Loesch, D. P., Perry, J. A., Heard-Costa, N. L., Taliun, D., Cade, B. E., Wang, H.,
764 Daya, M., Ziniti, J., Datta, S., Celedón, J. C., Soto-Quiros, M. E., Avila, L., Weiss, S. T.,
765 Barnes, K., Redline, S. S., Vasan, R. S., Johnson, A. D., Mathias, R. A., … Zoellner, S.
766 (2020). De novo mutations across 1,465 diverse genomes reveal mutational insights
767 and reductions in the Amish founder population. *Proceedings of the National Academy*
768 *of Sciences*, *117*(5), 2560–2569. https://doi.org/10.1073/pnas.1902766117
769 Kim, B. Y., Huber, C. D., & Lohmueller, K. E. (2017). Inference of the distribution of selection
770 coefficients for new nonsynonymous mutations using large samples. *Genetics*, *206*(1),
771 345–361. https://doi.org/10.1534/genetics.116.197145
772 Kim, Y. (2006). Allele frequency distribution under recurrent selective sweeps. *Genetics*,
773 *172*(3), 1967–1978. https://doi.org/10.1534/genetics.105.048447
774 Kim, Y., & Stephan, W. (2000). Joint Effects of Genetic Hitchhiking and Background Selection
775 on Neutral Variation. *Genetics*, *155*(3), 1415–1427.
776 https://doi.org/10.1093/genetics/155.3.1415
777 Kim, Y., & Stephan, W. (2002). Detecting a local signature of genetic hitchhiking along a
778 recombining chromosome. *Genetics*, 160, 765-777.
779 https://doi.org/10.1093/genetics/160.2.765
780 Kimura, M. (1968). Evolutionary rate at the molecular level. *Nature*, *217*(5129), 624–626.
781 https://doi.org/10.1038/217624a0
782 Kimura, M. (1983). *The Neutral Theory of Molecular Evolution* (1st ed.). Cambridge
783 University Press. https://doi.org/10.1017/CBO9780511623486
784 Kong, A., Thorleifsson, G., Gudbjartsson, D. F., Masson, G., Sigurdsson, A., Jonasdottir, A.,
785 Walters, G. B., Jonasdottir, A., Gylfason, A., Kristinsson, K. Th., Gudjonsson, S. A., Frigge,
786 M. L., Helgason, A., Thorsteinsdottir, U., & Stefansson, K. (2010). Fine-scale
787 recombination rate differences between sexes, populations and individuals. *Nature*,
788 *467*(7319), 1099–1103. https://doi.org/10.1038/nature09525
789 Kousathanas, A., & Keightley, P. D. (2013). A comparison of models toi the distribution of
790 fitness effects of new mutations. *Genetics*, *193*(4), 1197–1208.
791 https://doi.org/10.1534/genetics.112.148023
792 Lewontin, R. C. (1987). Polymorphism and heterosis: Old wine in new bottles and vice versa.
793 *Journal of the History of Biology*, *20*(3), 337–349. https://doi.org/10.1007/BF00139459
794 Li, H., & Stephan, W. (2006). Inferring the demographic history and rate of adaptive
795 substitution in *Drosophila*. *PLoS Genetics*, *2*(10), e166.
796 https://doi.org/10.1371/journal.pgen.0020166
797 Matuszewski, M., Hildebrandt, M., Achaz, G., & Jensen, J.D. (2018). Coalescent processes
798 with skewed offspring distributions and non-equilibrium demography. *Genetics,* 208,
799 323-38.
800 https://doi.org/10.1534/genetics.117.300499
801 Maynard Smith, J., & Haigh, J. (1974). The hitch-hiking effect of a favourable gene. *Genetical*
802 *Research*, *23*(1), 23–35. https://doi.org/10.1017/S0016672300014634
803 McVicker, G., Gordon, D., Davis, C., & Green, P. (2009). Widespread genomic signatures of
804 natural selection in hominid evolution. *PLoS Genetics*, *5*(5), e1000471.
805 https://doi.org/10.1371/journal.pgen.1000471

Mellars, P. (2006). Why did modern human populations disperse from Africa *ca.* 60,000 years ago? A new model. *Proceedings of the National Academy of Sciences*, *103*(25), 9381–9386. https://doi.org/10.1073/pnas.0510792103

Messer, P. W., & Petrov, D. A. (2013). Frequent adaptation and the McDonald-Kreitman test. *Proceedings of the National Academy of Sciences of the United States of America*, *110*(21), 8615–8620. https://doi.org/10.1073/pnas.1220835110

Miles, A., Rodrigues, M.F., Ralph, P., Kelleher, J., Schelker, M., Pisupati, R., Rae, S., & Millar, T. (2024). *scikit-allel: V1.3.8* (v1.3.8) #. https://doi.org/10.5281/ZENODO.10876220

Moorjani, P., Amorim, C. E. G., Arndt, P. F., & Przeworski, M. (2016). Variation in the molecular clock of primates. *Proceedings of the National Academy of Sciences*, *113*(38), 10607–10612. https://doi.org/10.1073/pnas.1600374113

Morales-Arce, A. Y., Johri, P., & Jensen, J. D. (2022). Inferring the distribution of fitness effects in patient-sampled and experimental virus populations: Two case studies. *Heredity*, *128*(2), 79–87. https://doi.org/10.1038/s41437-021-00493-y

Nicolaisen, L. E., & Desai, M. M. (2013). Distortions in genealogies due to purifying selection and recombination. *Genetics*, *195*(1), 221–230. https://doi.org/10.1534/genetics.113.152983

Nielsen, R. (2005). Molecular Signatures of Natural Selection. *Annual Review of Genetics*, *39*(1), 197–218. https://doi.org/10.1146/annurev.genet.39.073003.112420

Nielsen, R., Williamson, S., Kim, Y., Hubisz, M. J., Clark, A. G., & Bustamante, C. (2005). Genomic scans for selective sweeps using SNP data. *Genome Research*, *15*(11), 1566–1575. https://doi.org/10.1101/gr.4252305

Pavlidis, P., Jensen, J. D., & Stephan, W. (2010). Searching for Footprints of Positive Selection in Whole-Genome SNP Data From Nonequilibrium Populations. *Genetics*, *185*(3), 907–922. https://doi.org/10.1534/genetics.110.116459

Pollard, K. S., Hubisz, M. J., Rosenbloom, K. R., & Siepel, A. (2010). Detection of nonneutral substitution rates on mammalian phylogenies. *Genome Research*, *20*(1), 110–121. https://doi.org/10.1101/gr.097857.109

Poh, Y.-P., Domingues, V., Hoekstra, H.E., & Jensen, J.D. (2014). On the prospect of identifying adaptive loci in recently bottlenecked populations. *PLoS One,* 9(11), e110579. https://doi.org/10.1371/journal.pone.0110579

Przeworski, M., (2002). The signature of postive selection at randomly chosen loci. *Genetics*, 160, 1179-1189. https://doi.org/10.1093/genetics/160.3.1179

Sackman, A., Harris, R., & Jensen, J.D. (2019). Inferring demography and selection in organisms characterized by skewed offspring distributions. *Genetics,* 211, 1019-28. https://doi.org/10.1534/genetics.118.301684

Sakharkar, M. K., Chow, V. T. K., & Kangueane, P. (2004). Distributions of exons and introns in the human genome. *In Silico Biology*, *4*(4), 387–393.

Sayers, E. W., Bolton, E. E., Brister, J. R., Canese, K., Chan, J., Comeau, D. C., Connor, R., Funk, K., Kelly, C., Kim, S., Madej, T., Marchler-Bauer, A., Lanczycki, C., Lathrop, S., Lu, Z., Thibaud-Nissen, F., Murphy, T., Phan, L., Skripchenko, Y., … Sherry, S. T. (2022). Database resources of the national center for biotechnology information. *Nucleic Acids Research*, *50*(D1), D20–D26. https://doi.org/10.1093/nar/gkab1112

Schiffels, S., & Durbin, R. (2014). Inferring human population size and separation history from multiple genome sequences. *Nature Genetics*, *46*(8), 919–925. https://doi.org/10.1038/ng.3015

Schneider, A., Charlesworth, B., Eyre-Walker, A., & Keightley, P. D. (2011). A Method for inferring the rate of occurrence and fitness effects of advantageous mutations. *Genetics*, *189*(4), 1427–1437. https://doi.org/10.1534/genetics.111.131730

Schrider, D. R., Shanku, A. G., & Kern, A. D. (2016). Effects of linked selective sweeps on demographic inference and model selection. *Genetics*, *204*(3), 1207–1223. https://doi.org/10.1534/genetics.116.190223

Siepel, A., Bejerano, G., Pedersen, J. S., Hinrichs, A. S., Hou, M., Rosenbloom, K., Clawson, H., Spieth, J., Hillier, L. W., Richards, S., Weinstock, G. M., Wilson, R. K., Gibbs, R. A., Kent, W. J., Miller, W., & Haussler, D. (2005). Evolutionarily conserved elements in vertebrate, insect, worm, and yeast genomes. *Genome Research*, *15*(8), 1034–1050. https://doi.org/10.1101/gr.3715005

Simkin, A., Bailey, J., Theurkauf, B., Gao, F.-B., & Jensen, J.D. (2014). Inferring the evolutionary history of primate miRNA binding sites: overcoming motif counting biases. *Molecular Biology & Evolution,* 31, 1894-1901. https://doi.org/10.1093/molbev/msu129

Soni, V., & Jensen, J. D. (2024). Temporal challenges in detecting balancing selection from population genomic data. *G3: Genes, Genomes, Genetics, 14*(6), jkae069. https://doi.org/10.1093/g3journal/jkae069

Soni, V., Terbot, J., & Jensen, J.D. (2024a). Population genetic considerations regarding the interpretation of within-patient SARS-CoV-2 polymorphism data. *Nature Communications,* 15, 3240. https://doi.org/10.1038/s41467-024-46261-4

Soni, V., Johri, P., & Jensen, J. D. (2023). Evaluating power to detect recurrent selective sweeps under increasingly realistic evolutionary null models. *Evolution*, qpad120. https://doi.org/10.1093/evolut/qpad120

Soni, V., Pfeifer, S. P., & Jensen, J. D. (2024b). The effects of mutation and recombination rate heterogeneity on the inference of demography and the distribution of fitness effects. *Genome Biology and Evolution*, *16*(2), evae004. https://doi.org/10.1093/gbe/evae004

Soni, V., Terbot, J. W., Versoza, C. J., Pfeifer, S. P., & Jensen, J. D. (2024c). A whole-genome scan for evidence of recent positive and balancing selection in aye-ayes (*Daubentonia madagascariensis*) utilizing a well-fit evolutionary baseline model. In preprint, BioRxiv. https://www.biorxiv.org/content/10.1101/2024.11.08.622667v1

Stephan, W. (1995). Perturbation analysis of a two-locus model with directional selection and recombination. *Journal of Mathematical Biology*, *34*(1), 95–109. https://doi.org/10.1007/BF00180138

Tajima, F. (1989). Statistical method for testing the neutral mutation hypothesis by DNA polymorphism. *Genetics*, *123*(3), 585–595.

Tataru, P., & Bataillon, T. (2020). polyDFE: Inferring the distribution of fitness effects and properties of beneficial mutations from polymorphism data. In J. Y. Dutheil (Ed.), *Statistical Population Genomics* (Vol. 2090, pp. 125–146). Springer US. https://doi.org/10.1007/978-1-0716-0199-0_6

Tennessen, J. A., Bigham, A. W., O'Connor, T. D., Fu, W., Kenny, E. E., Gravel, S., McGee, S., Do, R., Liu, X., Jun, G., Kang, H. M., Jordan, D., Leal, S. M., Gabriel, S., Rieder, M. J.,

Abecasis, G., Altshuler, D., Nickerson, D. A., Boerwinkle, E., … NHLBI Exome Sequencing Project. (2012). Evolution and functional impact of rare coding variation from deep sequencing of human exomes. *Science (New York, N.Y.), 337*(6090), 64–69. https://doi.org/10.1126/science.1219240

Terbot, J., Cooper, B., Good, J, & Jensen, J.D. (2023a). A simulation framework for modeling the within-patient evolutionary dynamics of SARS-CoV-2. *Genome Biology & Evolution,* 15, evad204. https://doi.org/10.1093/gbe/evad204

Terbot, J. W., Johri, P., Liphardt, S. W., Soni, V., Pfeifer, S. P., Cooper, B. S., Good, J. M., & Jensen, J. D. (2023b). Developing an appropriate evolutionary baseline model for the study of SARS-CoV-2 patient samples. *PLOS Pathogens*, *19*(4), e1011265. https://doi.org/10.1371/journal.ppat.1011265

Terbot, J. W., Soni, V., Versoza, C. J., Pfeifer, S. P., & Jensen, J. D. (2024). Inferring the demographic history of aye-ayes (*Daubentonia madagascariensis*) from high-quality, whole-genome, population-level data. In preprint, BioRxiv. https://www.biorxiv.org/content/10.1101/2024.11.08.622659v1

Terhorst, J., Kamm, J. A., & Song, Y. S. (2017). Robust and scalable inference of population history from hundreds of unphased whole genomes. *Nature Genetics*, *49*(2), 303–309. https://doi.org/10.1038/ng.3748

The 1000 Genomes Project Consortium. (2015). A global reference for human genetic variation. *Nature*, *526*(7571), 68–74. https://doi.org/10.1038/nature15393

Thornton, K. (2003). libsequence: A C++ class library for evolutionary genetic analysis. *Bioinformatics*, *19*(17), 2325–2327. https://doi.org/10.1093/bioinformatics/btg316

Wang, K., Mathieson, I., O'Connell, J., & Schiffels, S. (2020). Tracking human population structure through time from whole genome sequences. *PLOS Genetics*, *16*(3), e1008552. https://doi.org/10.1371/journal.pgen.1008552

Wang, R. J., Al-Saffar, S. I., Rogers, J., & Hahn, M. W. (2023). Human generation times across the past 250,000 years. *Science Advances*, *9*(1), eabm7047. https://doi.org/10.1126/sciadv.abm7047

Wiehe, T. H. E., & Stephan, W. (1993). Analysis of a genetic hitchhiking model, and its application to DNA polymorphism data from Drosophila melanogaster. *Molecular Biology and Evolution*. https://doi.org/10.1093/oxfordjournals.molbev.a040046

Williamson, S. H., Hernandez, R., Fledel-Alon, A., Zhu, L., Nielsen, R., & Bustamante, C. D. (2005). Simultaneous inference of selection and population growth from patterns of variation in the human genome. *Proceedings of the National Academy of Sciences*, *102*(22), 7882–7887. https://doi.org/10.1073/pnas.0502300102

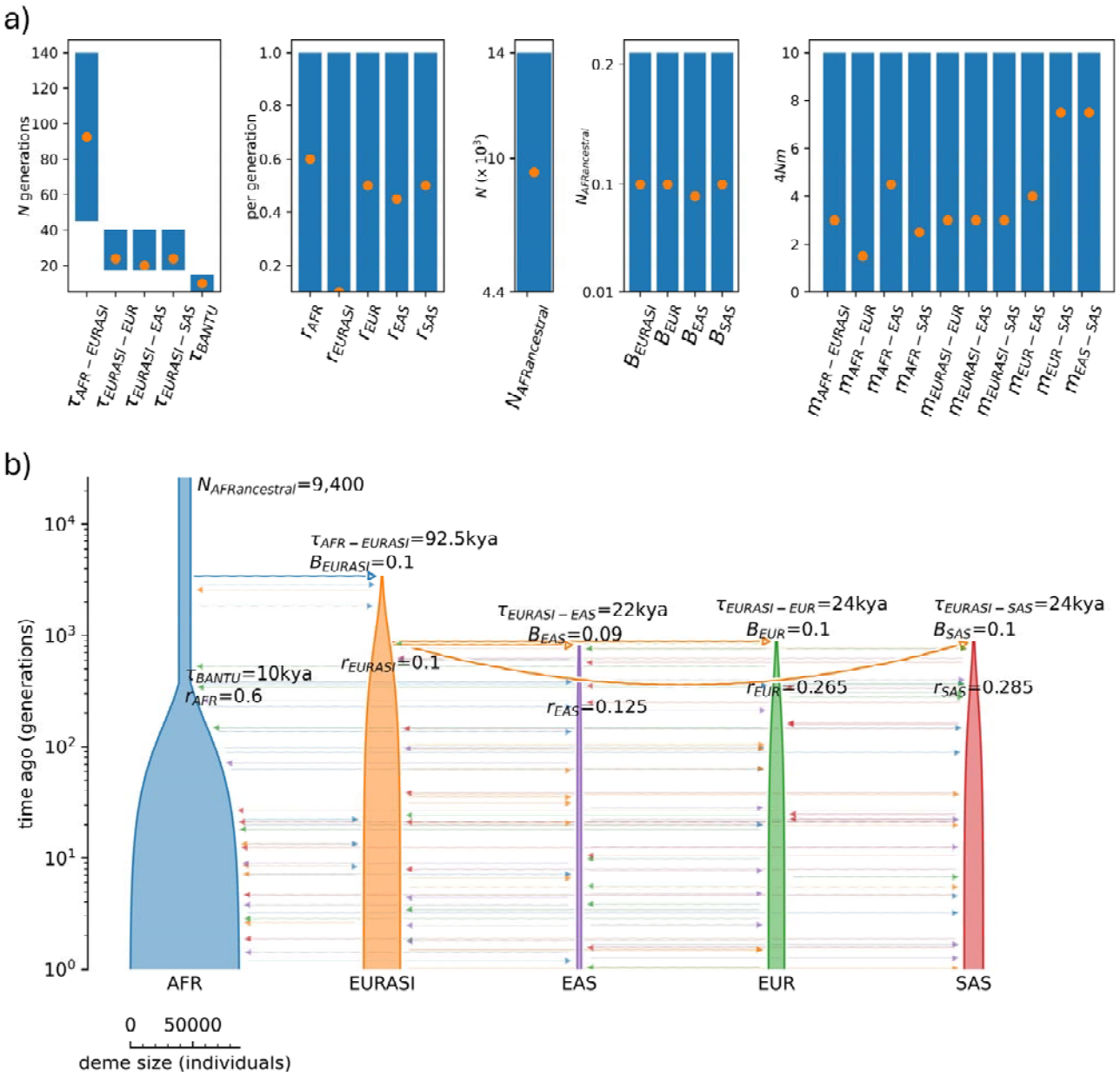

Figure 1: Demographic model representing the Out-of-Africa expansion. a) Parameter ranges for all 25 parameters (represented by the blue bars on the plots). Orange dots indicate the best fitting parameter values identified. b) Plot of demographic model with the best fitting parameter values. Population key: AFRancestral = initial ancestral African population; AFR = African population; EURASI = unsampled Eurasian population; EUR = European population; EAS = East Asian population; SAS = South Asian population. Parameter key: τ = time of splits between specified populations (with τ_{BANTU} representing the time of start of the Bantu expansion in the African population); r = growth parameter; N = population size; B = bottleneck severity; m = migration rate. Demographic model graphic generated using Demes software (Gower et al. 2022).

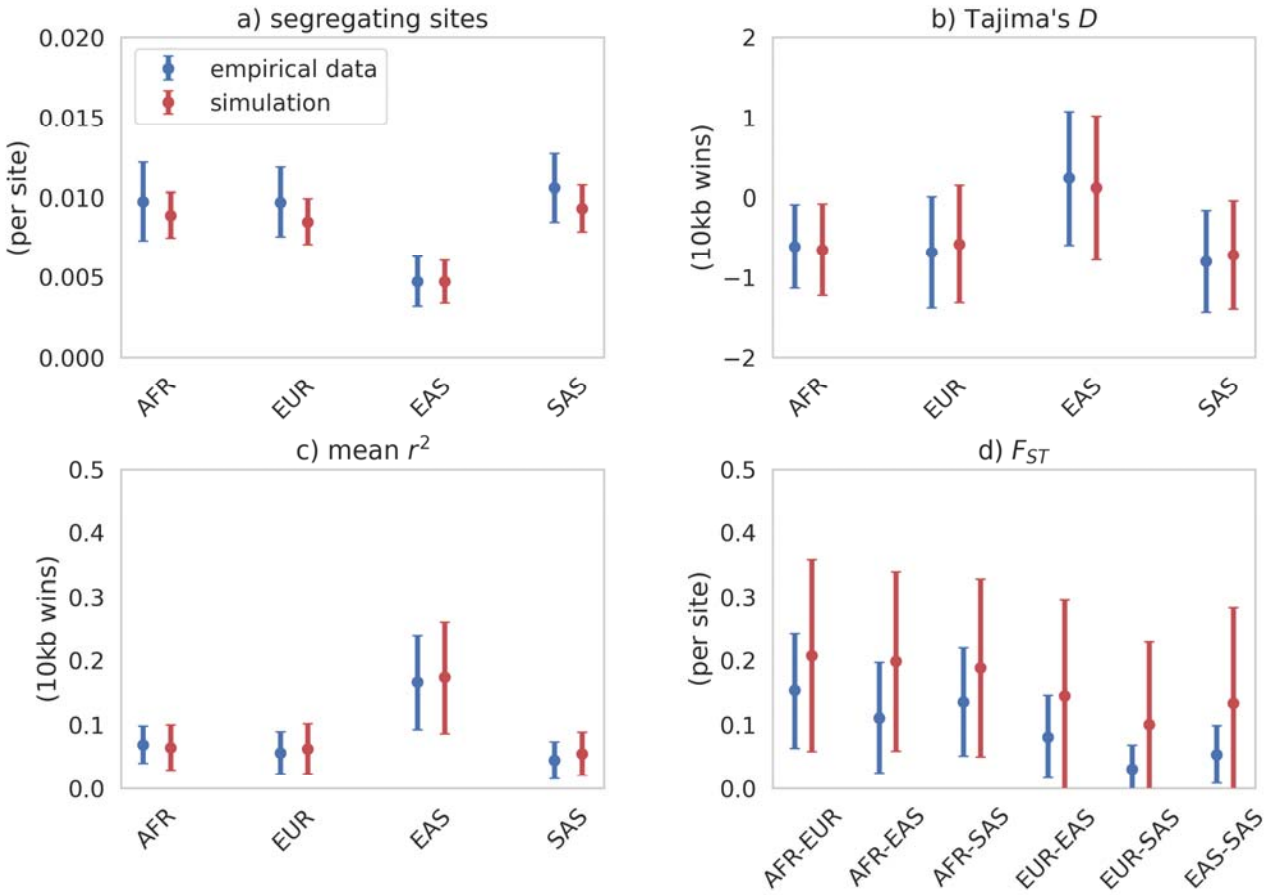

Figure 2: Summary statistics calculated from putatively neutral non-functional regions from population samples for empirical (blue) data, compared to simulated (red) data under the best-fitting demographic model. Means and standard deviations were calculated for 100 replicates. Data points represent the mean across regions, while bars represent the mean of the standard deviations across all regions.

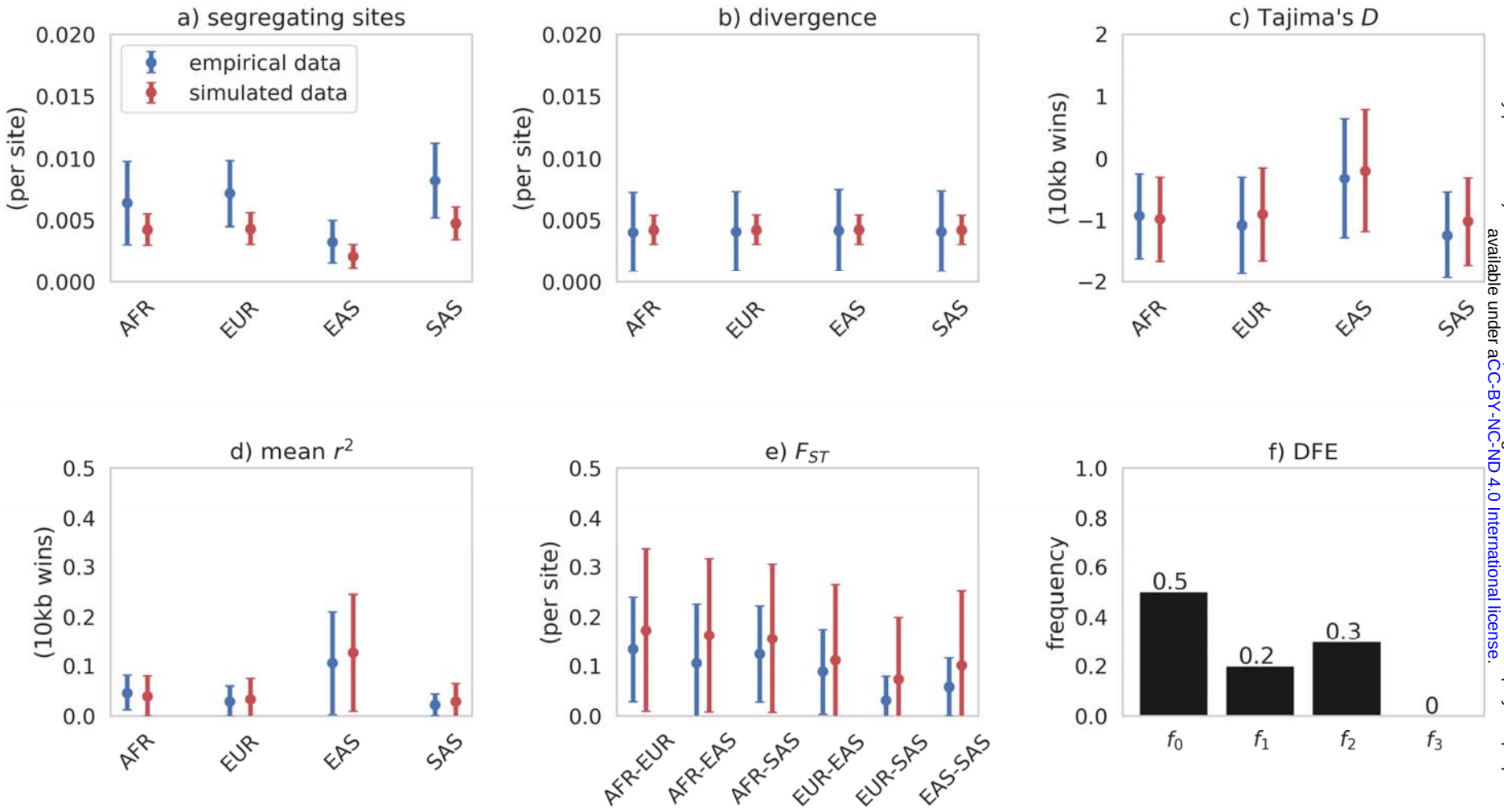

Figure 3: a) to e) Summary statistics calculated from functional regions from population samples for empirical (blue) data, compared to simulated (red) data under the best-fitting neutral demographic model with the addition of purifying and background selection modelled using

the Johri et al. (2023) DFE (shown in panel f). Following this DFE, exonic mutations were drawn from a DFE comprised of 4 fixed classes with frequencies denoted by f_i: f_0 with $0 \leq 2N_{AFRancestral}\, s < 1$ (i.e., effectively neutral mutations), f_1 with $1 \leq 2N_{AFRancestral}\, s < 10$ (i.e., weakly deleterious mutations), f_2 with $10 \leq 2N_{AFRancestral}l\, s < 100$ (i.e., moderately deleterious mutations), and f_3 with $100 \leq 2N_{AFRancestral}\, s$ (i.e., strongly deleterious mutations), where $N_{AFRancestral}$ was the initial population size and s the reduction in fitness of the mutant homozygote relative to wild-type. Means and standard deviations were calculated for 100 replicates. Data points represent the mean across regions, while bars represent the mean of the standard deviations across all regions.

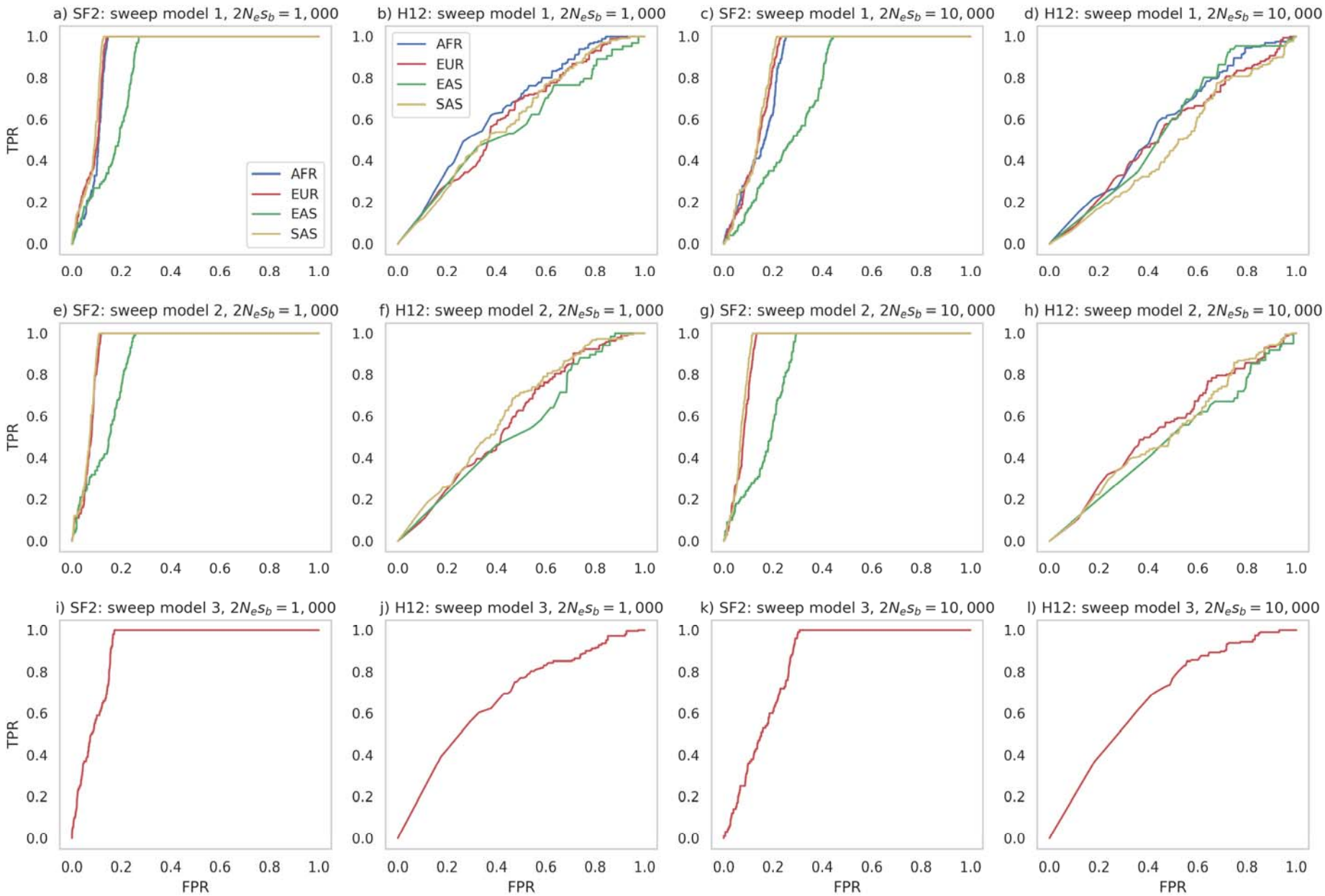

Figure 4: ROC curves, providing the change in true-positive rate (TPR) with false-positive rate (FPR), for sweep inference with SweepFinder2 (SF2) and the H12 statistic under the demographic model inferred in this study (see Figure 1) together with the Johri et al. (2023) DFE for functional regions, and variable mutation and recombination rates (see Methods section). Here, a single beneficial mutation was introduced into the population at three different time points and in three different populations: Model 1: the beneficial mutation was introduced into the ancestral African population immediately after the burn-in period, the beneficial fixation is present in all populations, and sweep inference was conducted on all sampled populations; Model 2: the beneficial mutation was introduced into the ancestral Eurasian population immediately upon splitting from the ancestral African population, the beneficial fixation is present in all non-African populations, and sweep inference was conducted on the European, East Asian and South Asian populations; Model 3: the beneficial mutation was introduced into the European population immediately upon splitting from the Eurasian population, the beneficial fixation is present in the European population, and sweep inference was conducted on this population only. For each model, two different strengths of selection were modelled: $2N_e s_b = 1{,}000$ and $2N_e s_b = 10{,}000$, where N_e is the size of the ancestral African population and s_b is the selection coefficient of the beneficial mutation. Inference with SweepFinder2 was performed on each SNP and substitution, whilst H12 inference was performed on each SNP over a 1kb window, with the SNP at the center of the window.